NeuroImage 277 (2023) 120264

Contents lists available at ScienceDirect

NeuroImage

journal homepage: www.elsevier.com/locate/ynimg

The maturation of aperiodic EEG activity across development reveals a progressive differentiation of wakefulness from sleep

Jacopo Favaro[a,1,*], Michele Angelo Colombo[b,1,*], Ezequiel Mikulan[b], Stefano Sartori[a,d,e], Margherita Nosadini[a,d], Maria Federica Pelizza[a], Mario Rosanova[b], Simone Sarasso[b], Marcello Massimini[b,c,2,*], Irene Toldo[a,2]

[a] Pediatric Neurology and Neurophysiology Unit, Department of Women's and Children Health, University of Padua, 35128, Padua, Italy
[b] Department of Clinical and Biomedical Sciences, University of Milan, 20157, Milan, Italy
[c] IRCCS, Fondazione Don Carlo Gnocchi Onlus, 20148, Milan, Italy
[d] Neuroimmunology Group, Pediatric Research Institute "Città della Speranza", 35127, Padua, Italy
[e] Department of Neuroscience, University of Padua, 35121, Padua, Italy

ARTICLE INFO

Keywords:
Functional brain development
1/f noise
EEG
Aperiodic activity
Sleep

ABSTRACT

During development, the brain undergoes radical structural and functional changes following a posterior-to-anterior gradient, associated with profound changes of cortical electrical activity during both wakefulness and sleep. However, a systematic assessment of the developmental effects on aperiodic EEG activity maturation across vigilance states is lacking, particularly regarding its topographical aspects. Here, in a population of 160 healthy infants, children and teenagers (from 2 to 17 years, 10 subjects for each year), we investigated the development of aperiodic EEG activity in wakefulness and sleep. Specifically, we parameterized the shape of the aperiodic background of the EEG Power Spectral Density (PSD) by means of the spectral exponent and offset; the exponent reflects the rate of exponential decay of power over increasing frequencies and the offset reflects an estimate of the y-intercept of the PSD.

We found that sleep and development caused the EEG-PSD to rotate over opposite directions: during wakefulness the PSD showed a flatter decay and reduced offset over development, while during sleep it showed a steeper decay and a higher offset as sleep becomes deeper. During deep sleep (N2, N3) only the spectral offset decreased over age, indexing a broad-band voltage reduction. As a result, the difference between values in deep sleep and those in both light sleep (N1) and wakefulness increased with age, suggesting a progressive differentiation of wakefulness from sleep EEG activity, most prominent over the frontal regions, the latest to complete maturation. Notably, the broad-band spectral exponent values during deep sleep stages were entirely separated from wakefulness values, consistently across developmental ages and in line with previous findings in adults. Concerning topographical development, the location showing the steepest PSD decay and largest offset shifted from posterior to anterior regions with age. This shift, particularly evident during deep sleep, paralleled the migration of sleep slow wave activity and was consistent with neuroanatomical and cognitive development.

Overall, aperiodic EEG activity distinguishes wakefulness from sleep regardless of age; while, during development, it reveals a postero-anterior topographical maturation and a progressive differentiation of wakefulness from sleep. Our study could help to interpret changes due to pathological conditions and may elucidate the neurophysiological processes underlying the development of wakefulness and sleep.

* Corresponding authors.
E-mail address: marcello.massimini@unimi.it (M. Massimini).
[1] These authors contributed equally to this work.
[2] These are co-senior authors.

https://doi.org/10.1016/j.neuroimage.2023.120264.
Received 7 March 2023; Received in revised form 4 June 2023; Accepted 1 July 2023
Available online 1 July 2023.

1. Introduction

1.1. Region-specific synaptic remodeling and myelination

During the first years of life, the brain undergoes radical structural changes, including modifications of connections with progressively increasing degrees of complexity (Silbereis et al., 2016). The full-term newborn brain has many more synapses than the adult brain and during infancy a period of intense synaptogenesis is followed by a phase of synaptic pruning (Casey et al., 2005). Interestingly, the time course for this synaptic remodeling is region-specific, with the peak of synaptic overproduction occurring at different times depending on the brain region (Casey et al., 2005; Toga et al., 2006; Tamnes et al., 2010), following a postero-anterior gradient. Another fundamental process is white matter formation, which also proceeds from posterior to anterior regions and from central to peripheral locations during the first two years of age (Barkovich et al., 1988; Ballesteros et al., 1993; Welker and Patton, 2012). The development of GABAergic function strongly influences these processes, as GABA levels increase during early development, reach a plateau during adolescence, and slowly decrease with aging (Porges et al., 2021). GABA receptor expression may facilitate synaptic pruning (Afroz et al., 2016) and the GABAergic system is linked to myelination by controlling oligodendrocyte precursor cell activity (Vélez-Fort et al., 2012). These region and time-specific changes in GABAergic function and the subsequent shift in the balance between glutamate and GABA levels are also fundamental in inducing neuroplasticity during critical periods of neurodevelopment and acquiring new cognitive abilities (Hensch, 2005; Cohen Kadosh et al., 2015). All these processes are reflected in a profound modification of cortical electrophysiology.

1.2. Maturation of periodic EEG activity during development in wakefulness and sleep

Neural oscillations are the most prominent feature of EEG activity; they are observed throughout the nervous system at multiple spatial and temporal scales (Varela et al., 2001) and they seem to be ubiquitous across species (Buzsáki and Draguhn, 2004).

In humans, bursts of periodic oscillations with variable frequency emerge spontaneously in the first year of life, alternating with stretches of aperiodic activity (Schaworonkow and Voytek, 2021). Starting from the 3rd-4th month of life a rhythmic, nearly regular, electrical activity at 3–4 Hz (delta) emerges on the posterior regions, progressively increasing in frequency until reaching 5–7 Hz (theta) at 12 months (Smith, 2012). During neurodevelopment, these periodic rhythms will be further reorganized into the 8–13 Hz activity, namely the posterior alpha rhythm and the *mu* sensori-motor rhythm, commonly observed in the EEG of children and adults. Paralleling neuroanatomical development, waking delta, theta and alpha EEG band oscillations develop first at the occipital level and only later at the parietal, central and frontal level (Gasser et al., 1988). Moreover, following the same spatial gradient over time, alpha replaces theta activity, most rapidly in occipital regions (Benninger et al., al.,1984). These changes of EEG rhythmic activity seem to parallel the development of sensory, motor and cognitive systems (Varela et al., 2001).

Related to sleep, a milestone study from Kurth et al. (2010) mapped cortical activity during the first two decades of life. The main finding of the study is that the location with maximal slow wave activity (SWA) undergoes a shift from posterior to anterior regions across childhood and adolescence. A maturation along a postero-anterior axis has been recently shown also for sleep spindles (Kwon et al., 2023). Regarding the spectral profile in NREM sleep, the highest power was observed in the SWA range across all age groups from 2 to 20 years old; moreover, the power of all frequency ranges decreases over development.

1.3. Maturation of aperiodic EEG activity during development in wakefulness and sleep

Also the background aperiodic (i.e. non-oscillatory) activity undergoes developmental changes in wakefulness and sleep, bearing important cognitive relevance (Voytek et al., 2015; Tran et al., 2020; Ostlund et al., 2021). Research of the EEG Power Spectral Density (PSD) has traditionally focused on narrow-band power in classical frequency bands but conflating periodic and aperiodic or quasi-periodic activity (Donoghue et al., 2022; Palva and Palva, 2018). In this perspective, aperiodic activity should be studied separately from periodic activity in quantitative terms to gain understanding on brain development (Ostlund et al., 2022; Schaworonkow and Voytek, 2021; Cellier et al., 2021; Trondle et al., 2022).

The aperiodic background of the PSD (i.e. the 1/f-like component beneath the peaks corresponding to periodic activity) decays from slower to faster frequencies, according to an inverse power-law, with a 1/f-like shape (Pritchard, 1992; He et al., 2010). This relation can be expressed by two parameters: while the *spectral exponent* indexes the decay of the PSD, thus the relative expression of low and high frequencies, the *offset* reflects the power at long-time scales, strictly related to the global *power* of the aperiodic signal (Donoghue et al., 2020). Aperiodic activity is altered in various neuropsychiatric pathological conditions, such as neurodevelopmental disorders, schizophrenia, epilepsy and disorders of consciousness (Pani et al., 2022).

Various recent longitudinal and cross-sectional studies have already investigated the maturation of the above-described components in wakefulness (Cellier et al., 2021; McSweeney et al., 2021; Schaworonkow and Voytek, 2021; Ostlund et al., 2021; Hill et al., 2022; Trondle et al., 2022) also relating them to complexity measures like multiscale entropy (Van Noortd and Willoughby, 2021). However they used low sample numbers or non-homogeneous populations to study broad age ranges and very large populations to study narrow age ranges.

Moreover, a growing number of reports on sleep-related changes in aperiodic EEG activity in adult and pediatric populations (Miskovic et al., 2019; Lendner et al., 2020; Bódizs et al., 2021) have recently been published. As an example, a large comprehensive study on children, adolescents and adults demonstrates that the spectral exponent could be a robust index of sleep stages across development (Schneider et al., 2022). Although the study results appear promising, they are limited by the lack of subjects below the age of 4 and by the application of the same sleep scoring rules in children and adults. Another recent study (Horvath et al., 2022) reports that both aperiodic and periodic components undergo remarkable overnight changes: during consecutive sleep cycles, a PSD rotation (a flatter decay and a smaller intercept) is observed. Consequently, the spectral exponent behaves similarly to the classical SWA yet it seems more promising because its interindividual variability is lower.

Finally, a very recent study explores in depth the relationship between age and aperiodic activity in a large pediatric population in wakefulness, by means of multilevel models (McSweeney et al., 2023). This study underlines the need to compare aperiodic activity maturation across infancy and childhood in wakefulness and in sleep states: our study develops exactly from this point.

1.4. Aims and hypothesis of the study

The first aim is to investigate the maturation during development of the aperiodic component of the EEG signal in wakefulness with a homogeneous coverage of each year of age. We hypothesize a counterclockwise PSD rotation (i.e. flatter PSD decay and lower PSD offset) over development (Cellier et al., 2021; McSweeney et al., 2021; Schaworonkow and Voytek, 2021). Moreover, we investigate the same maturation in sleep, in a subset of subjects that reached N3 sleep during a nap opportunity. We hypothesize that the PSD rotates clockwise as sleep deepens (Miskovic et al., 2019; Schneider et al., 2022), and coun-

terclockwise over development, within each sleep stage (Bódizs et al., 2021). We also aim to map these age-related changes of the aperiodic activity in wakefulness and sleep, an aspect ignored by previous studies. According to the posterior-to-anterior gradient of structural development (Casey et al., 2005; Welker and Patton, 2012), we hypothesize that the hot-spot where the aperiodic component is slowest (i.e. steepest PSD decay and largest PSD offset) migrates from posterior to anterior sites with increasing age, particularly during sleep.

The second aim is to assess how the aperiodic features of EEG activity diverge between wakefulness and sleep stages over age. We hypothesize an increasing divergence throughout development.

2. Material and methods

An analytical observational, retrospective, monocentric study was conducted - in accordance with the Declaration of Helsinki and the institutional guidelines - at the Pediatric Neurology and Neurophysiology Unit of the Department of Women's and Child Health of the University of Padua in collaboration to the Department of Clinical and Biomedical Sciences of the University of Milan, Italy. The study protocol was approved by the Ethics Committee for Clinical Trials of the University Hospital of Padua (protocol number AOP2091_33806)

2.1. Subjects, inclusion and exclusion criteria

We selected a large study population, covering uniformly a wide age range. Such a high sample number was obtained by recruiting subjects who underwent EEG at the Pediatric Neurology and Neurophysiology Unit of the Department of Women's and Child Health of the University of Padua from 2013 to 2020 after a paroxysmal event. Once the non-epileptic nature of the event has been ascertained, subjects were recruited on the base of the following inclusion and exclusion criteria:

Inclusion criteria*:* age at EEG recording between 2 and 17 years*;* typical neurodevelopment and no ongoing neurological issues; EEG signal obtained by 19 recording electrodes positioned according to the international system 10–20*;* normal EEG tracings; the presence of at least 5 min of quiet wakefulness free of artifacts; if the sleep phase was reached, the presence of at least 5 min of NREM sleep (N2-N3 phase).

Exclusion criteria*:* a pathological EEG in the previous 6 months; diagnosis of a neurological condition, neurodevelopmental disorder or psychiatric disease*;* ongoing therapy with benzodiazepines, phenobarbital, steroids or other drugs potentially interfering with the EEG signal.

For the determination of aperiodic features in wakefulness, we enrolled 10 subjects for each year of age (from 2 to 17 years), for a total of 160 subjects and as many EEG tracings. Sleep EEG was available in 89/160 subjects but only those subjects who reached the N3 phase of NREM sleep ($n = 44$) were considered.

The recordings lasted either 20 min (if recorded only during wakefulness, $n = 71$) or 60 min (if after wakefulness a sleep opportunity was given, $n = 89$). During wakefulness the subjects are sitting on a comfortable chair or in the arms of the parent and do not perform any particular task, except alternating periods of dozens of seconds with eyes open and with eyes closed (with a constant protocol across subjects). When necessary, younger children watched TV cartoons in order to improve compliance and reduce motion artifacts. EEG recordings were performed after acquiring a written informed consent from the subjects' parents; data were fully anonymized.

2.2. Data acquisition and pre-processing

Each EEG tracing was obtained by 19 recording electrodes (cup in chlorinated silver) positioned according to the international 10–20 system and a 40-channel amplifier (Galileo MIZAR - Sirius, EBNeuro, Florence, Italy). In acquisition, an additional electrode located between the F3 and F4 electrodes was used as a reference; the impedances of all the electrodes were kept below 5 kΩ for the entire duration of the recording. The signal was filtered online during acquisition (0.1–70 Hz) and sampled at 256 Hz.

The raw data were imported and analyzed with custom MATLAB code (MATLAB 9.7.0 R2019b, The MathWorks Inc., Natick, MA, USA).

The signal was filtered by a 5th order Butterworth high pass filter at 0.5 Hz, a 3rd order Butterworth low-pass filter at 60 Hz and a 50 Hz Notch filter. Due to the low-density set-up and the careful application of electrodes, recordings from all electrodes were deemed of sufficiently good quality, resulting in no rejection of electrodes. Epochs characterized by artifacts were visually selected and excluded by a pediatric neurologist expert in EEG (JF). The waking and sleep epochs were also manually selected; sleep epochs were scored according to the most recent manual of the American Academy of Sleep Medicine (Iber et al., 2007), into four stages (Wakefulness, N1, N2, N3). Data were then re-referenced to the average reference.

In addition, to minimize the influence of electromyographic (EMG) and electro-oculographic (EOG) activity, an Independent Component Analysis was performed separately for wakefulness and sleep: the different components of the signal were visually inspected on the basis of their time-series, topographies and PSD. Clearly identifiable components of EMG and EOG activity were removed. The residual components were back-projected into the electrodes space.

We reported in Supplementary Table 1 and Supplementary Table 2 the proportion of epochs and the median number of components rejected for each vigilance stage. We performed both a correlation analysis with age and a partial correlation analysis to ensure that these factors did not contribute to the results (see **2.6.6 Control analyses** and **3 Results**).

2.3. Calculation of aperiodic features: spectral exponent and offset

The PSD was estimated using Welch's method, with a 3 second Hanning window and a 50% overlap. The linear trend of the time-series within each window was removed to avoid introducing very slow frequencies that can bias the power estimate.

We estimated the spectral exponent and offset respectively from the slope and the intercept of the linear relationship between the logarithm of the PSD and the logarithm of frequency, after discarding frequency bins displaying oscillatory peaks (i.e. bins with large positive residuals from a preliminary linear fit, and their contiguous bins with positive residuals). Details of the procedure have been published in Colombo et al., 2019 and the code is available online at: https://github.com/milecombo/spectralExponent/blob/master/README.md.

Specifically, our fitting algorithm first resamples the PSD over log-spaced frequency bins (to ensure the lower frequencies are adequately represented and leveraged with respect to the higher frequencies, by up-sampling), then performs a preliminary linear fit (in log-log axes), then identifies peaks (large residuals from the preliminary fit, > 2 median absolute deviations, also displaying a peak/inflection point) along with the base of the peaks (frequency bins with positive residuals adjacent to peaks), and fits again the PSD, after discarding the identified peaks, finally resulting in an intercept (spectral offset) and slope (spectral exponent). Results concerning the PSD residuals, and the proportion of excluded frequency bins, corresponding to periodic activity are shown in Supplementary Fig. 1.

Here, to facilitate the comparison between the results of the spectral exponent and offset, we considered the spectral offset as the PSD intercept, and the spectral exponent as the PSD slope multiplied by −1, derived from this simple equation: $\log_{10}(\text{PSD}) = \text{intercept} + \text{slope}^{*}\log_{10}(\text{frequency})$.

Thus, in this formalism, the spectral exponent is equivalent to the parameter α of the equation: PSD $\sim 1/f^{\alpha}$ (as in Pritchard, 1992; Cellier et al., 2021; Shaworonkow and Voytek, 2021) such that a progressive decay of the PSD across frequencies is not indexed by negative spectral exponent values (as in Colombo et al., 2019; Gao, 2016), but by positive values. We estimated the aperiodic features for each vigi-

lance stage (Wakefulness, N1, N2, N3) considering the average across all scalp electrodes (for the main analysis), and then considering individual electrodes (for exploratory topographic analysis). Whereas higher spectral exponent indexes steeper decay rate of the PSD across frequencies, higher spectral offset indexes overall larger PSD across frequencies (Donoghue et al., 2020). We estimated the aperiodic features over the 1–20 Hz range (to minimize the influence of muscular artifacts), and further reported results over the 1–40 Hz range in the Supplementary Material, for comparison with previous literature.

Spectral exponent and intercept are two complementary parameters resulting from fitting the PSD 1/f-like behavior, capturing the phenomenon of PSD shift and PSD rotation. Whereas a change in spectral offset can occur in absence of a change in spectral slope (PSD shift), any change in exponent induces a corresponding change in offset, when the PSD is rotating around a fulcrum at a non-zero frequency (see a visual explanation here: https://github.com/fooof-tools/Visualizers#spectral-rotation). Hence, these two measures were tightly correlated, as expected [Supplementary Fig. 2, Wake: R (42)=0.837, N1: R(42)=0.791, N2: R(42)=0.642, N3: R(42)=0.759] and cannot generally be interpreted independently. We thereby consider both parameters in relation to age and discuss interesting dissociations.

2.4. Posterior-to-anterior difference in aperiodic features

To evaluate the posteroanterior gradient of aperiodic activity across vigilance stages, we computed for each spectral feature a posterior-to-anterior difference between the average value of a posterior (C3, Cz, C4, P3, P4, Pz, T3, T4, T5, T6, O1, O2) and an anterior (Fp1, Fp2, F3, F4, F7, F8, Fz) electrode cluster. A negative posteroanterior difference in spectral exponent indexed a steeper PSD decay in anterior regions; similarly, a negative posteroanterior difference in spectral offset indexed higher PSD intercept in anterior regions.

2.5. Variability and differences in aperiodic features among vigilance stages

To evaluate the differentiation of aperiodic activity across vigilance stages, we computed an overall measure of divergence across stages, as the mean absolute deviation in the aperiodic features across all the four stages. We then evaluated the pairwise stage differences in aperiodic activity, as the difference in the aperiodic features between each pair of vigilance stages (N1-W, N2-W, N3-W, N2-N1, N3-N1, N3-N2). We computed such overall variability and pairwise differences considering the scalp-average values (for the main analysis), and then considering individual electrodes (for exploratory topographic analysis).

2.6. Statistics

2.6.1. Correlation of age with aperiodic features, during wakefulness

First, to evaluate the maturation of wake aperiodic activity, we considered the entire sample of subjects during wakefulness, and assessed the Pearson Correlation between age and the two aperiodic features (spectral exponent and offset) at the scalp-average level, resulting in R statistics (degrees of freedom = 158, Fig. 1). Exploratory Pearson correlation analyses were also performed at the single electrode level, to qualitatively assess topographical differences (Fig. 1).

2.6.2. Rank-correlation of sleep depth with aperiodic features

All subsequent analyses were performed in the subset of subjects reaching N3 sleep. To qualitatively observe the development of the PSD shape during wake and sleep, we displayed the PSD, averaged by geometric mean, in each age group (age was grouped only for display), for each vigilance stage (Fig. 2).

Then, to evaluate the strength of an overall monotonic relationship between aperiodic activity and sleep depth, regardless of age (Miskovic et al., 2019; Schneider et al., 2022), we assessed the Spearman rank-correlation between the values of the two aperiodic features at the scalp-average level and the progression of vigilance stages—ranging from Wakefulness, through N1, N2, to N3—resulting in Rho statistics (degrees of freedom = 42, Fig. 3A and C, top).

2.6.3. Correlation of age with aperiodic features, in each vigilance stage

To evaluate the development of aperiodic activity during wake and sleep, we assessed the Pearson correlation between age and each aperiodic feature at the scalp-average level, in all 4 vigilance stages, resulting in R statistics (degrees of freedom = 42, Fig. 3B and D, top). We adjusted the P-values for multiple comparisons across vigilance stages according to Bonferroni-Hochberg procedure. Exploratory Pearson correlation analyses were also performed at the single electrode level, to qualitatively assess topographical differences (Fig. 3B and D, bottom).

In order to estimate whether the correlations observed during wakefulness were different from that of any sleep stage and if the correlations decreased over vigilance stages, we adopted a bootstrap procedure (see details in Supplementary material, par. **Evaluation of differences between wake and sleep stages in the magnitude of the correlations of age with aperiodic and spatial features).**

2.6.4. Correlation of age with postero-anterior differences in aperiodic features, in each sleep stage

To evaluate the development of the postero-anterior gradient of aperiodic activity during wake and sleep, we assessed the Pearson Correlation between age and the posterior-to-anterior difference of each aperiodic feature, in all 4 vigilance stages, resulting in R statistics (degrees of freedom = 42, Fig. 4 displays the spectral exponent, Supplementary Fig. 17 displays the spectral offset). We adjusted the P-values for multiple comparisons across vigilance stages according to Bonferroni-Hochberg procedure. To qualitatively observe the migration of the hot-spot with steeper PSD decay, we display the topography of the average spectral exponent in each age group, for each vigilance stage, in Fig. 4 (the topography of the average spectral offset in each age group, for each vigilance stage, is displayed in Supplementary Fig. 17).

In order to assess whether the vigilance stage affected the correlations between age and the postero-anterior difference of each aperiodic feature, we performed bootstrap analysis, as above (Supplementary material, par. **Evaluation of differences between wake and sleep stages, in the magnitude of the correlations of age with aperiodic and spatial features).**

2.6.5. Developmental differentiation of the vigilance stages

To evaluate the overall developmental variability of aperiodic activity across all the vigilance stages, we calculated the mean absolute deviation across the 4 vigilance stages in each aperiodic feature at the scalp-average level and correlated these values with age (Fig. 5).

To evaluate the developmental differentiation of aperiodic activity between specific vigilance stages, we then computed the difference between pairs of vigilance stages in the aperiodic features at the scalp-average level, and correlated these difference values with age (Fig. 5). We adjusted the P-values for multiple comparisons across all pairs of vigilance stages (6 pairwise differences resulting from 4 vigilance stages) according to Bonferroni-Hochberg procedure.

Exploratory Pearson correlation analyses were also performed at the single electrode level, to qualitatively assess topographical differences (Fig. 5).

2.6.6. Control analyses

We reported in the Supplementary Table 1 and in Supplementary Table 2 the proportion of epochs and the median number of components rejected for each vigilance stage, across several age groups. We compared the main results (the Pearson correlation between aperiodic features and age) to those of a partial correlation analysis, factoring out the variation in cleaning quality between subjects, to ensure that differences in cleaning quality did not contribute to the main results (Supplementary Material, paragraph **Data cleaning and control for potential biases across age**).

Then, in order to evaluate whether the results are influenced by differences in model fit quality across age, we also performed a thorough analysis of the goodness of fit. This revealed that goodness of fit was high across vigilance stages and age, that changes in goodness of fit across age were small and there was no evidence that the main findings were influenced by this factor, as tested through bootstrapped partial correlation analysis (Supplementary Material, paragraph **Goodness of Fit and control for potential biases across age**).

Finally, we corroborated results from our fitting procedure by performing supplementary analyses with a well-known procedure to estimate aperiodic features, the Fitting Oscillations and One-Over-F (FOOOF) toolbox (Donoghue et al., 2020). The two procedures yielded highly similar results and estimates of the aperiodic features (Supplementary Material, paragraph **Replication of main results with the FOOOF algorithm**).

3. Results

A total of 160 subjects (95 males) aged 2 to 17 years, including 10 subjects for each year of age, were recruited according to the inclusion and exclusion criteria.

The amount of muscle noise is considerably higher in infants due to frequent movements during wakefulness. This resulted in a larger number of epochs being excluded during wakefulness in younger subjects. We verified that the variation in cleaning quality across subjects did not contribute to the main results, by means of bootstrapped partial correlation analysis (Supplementary Material, paragraph **'Data cleaning and control for potential biases across age'**).

3.1. Development of aperiodic activity in wakefulness

We first evaluated the development of wake aperiodic activity. The spectral exponent of the 1–20 Hz range linearly decreased with age during wakefulness ($R = -0.823$, d.f. = 158, $P < 0.001$ [$p = 1.31^{-40}$], Supplementary Table 8); revealing stronger correlations at central and parieto-occipital electrodes (Fig. 1). Similarly, the spectral offset of the 1–20 Hz range linearly decreased with age during wakefulness ($R = -0.888$, $P < 0.001$ [$p = 4.72^{-55}$] Supplementary Table 8), revealing stronger correlations at central electrodes (Fig. 1).

Similar results were obtained for the spectral exponent ($R = -0.661$, $P < 0.001$ [$p = 1.87^{-21}$]) and offset ($R = -0.854$, $P < 0.001$ [$p = 1^{-46}$]) of the 1–40 Hz range (Supplementary Table 8, Supplementary Fig. 13).

The mean values of spectral exponent and offset and their standard deviation (std) for each year of age ($n = 10$ each) are reported in Supplementary Table 1.

Overall, the wake PSD rotated counterclockwise over age, resulting in a flatter spectral exponent and lower offset (Fig. 1).

3.2. Aperiodic activity and the monotonic relation with vigilance stages

We evaluated the monotonic relation between aperiodic activity and vigilance stages, in the subset of 44 subjects who reached the N3 phase of NREM sleep.

Each subject included in the sleep analysis had at least five minutes of consolidated NREM sleep (N2+N3). Among these subjects, we detail in the **Supplementary materials (par. Data cleaning and control for potential biases across age)** the recording length and the duration of data included in the analysis.

As observed in previous literature, there was a correlation between age and the macro-structure of NREM sleep, such that older subjects had a lower prevalence of N3 sleep (R(42)= −0.41, P-raw =0.0058) and conversely a higher prevalence of N2 sleep (R(42)= 0.364, P-raw =0.0151).

We accounted for this factor by considering N2 and N3 stages separately, rather than considering NREM sleep as a whole and then averaging across periodograms within each stage.

Overall, the PSD rotated clockwise from wakefulness to deep NREM sleep, regardless of age (Fig. 2, all panels), resulting in a steeper spectral exponent and higher offset.

Specifically, the spectral exponent of the 1–20 Hz range progressively increased from wakefulness to deep sleep, i.e. from wakefulness,

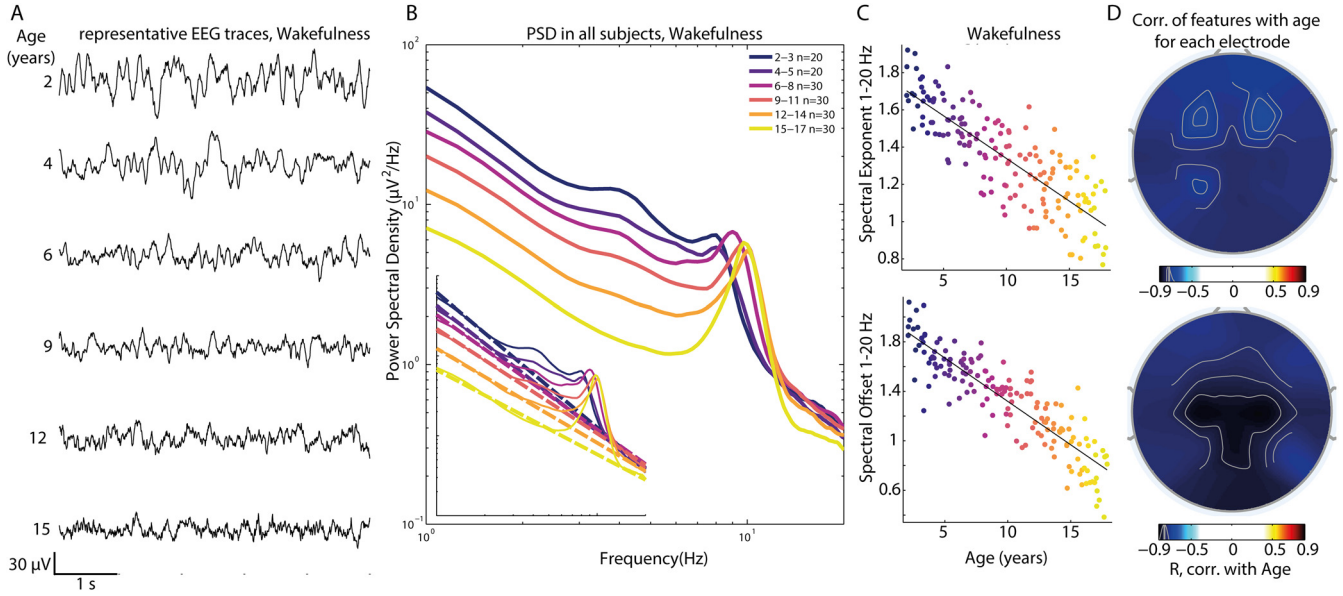

Fig. 1. During wakefulness, the PSD over the 1–20 Hz range rotates counterclockwise over the course of development, yielding lower spectral exponent and offset. A) Representative EEG traces for six subjects (aged 2, 4, 6, 12 and 15 years old), 5 s recorded from electrode Cz. Adolescents display lower amplitude and faster EEG. B) Geometric mean of the PSD taken first across electrodes, then across subjects that belonged to the same age group (numerosity is shown in the legend); grouping was performed for visual display only. The subpanel displays the PSD along with its 1/f-like trend, corresponding to the average fit of the aperiodic component. C) Correlations between age and each aperiodic feature at the scalp-average level, during wakefulness. Both the spectral exponent and the spectral offset of the 1–20 Hz range linearly decreased with age. D) The color-coded topographies of the correlations (ranging from blue, negative, to red, positive) reveal that the correlation between age and spectral exponent was stronger at central and parieto-occipital electrodes and the correlation between age and spectral offset was stronger at central electrodes.

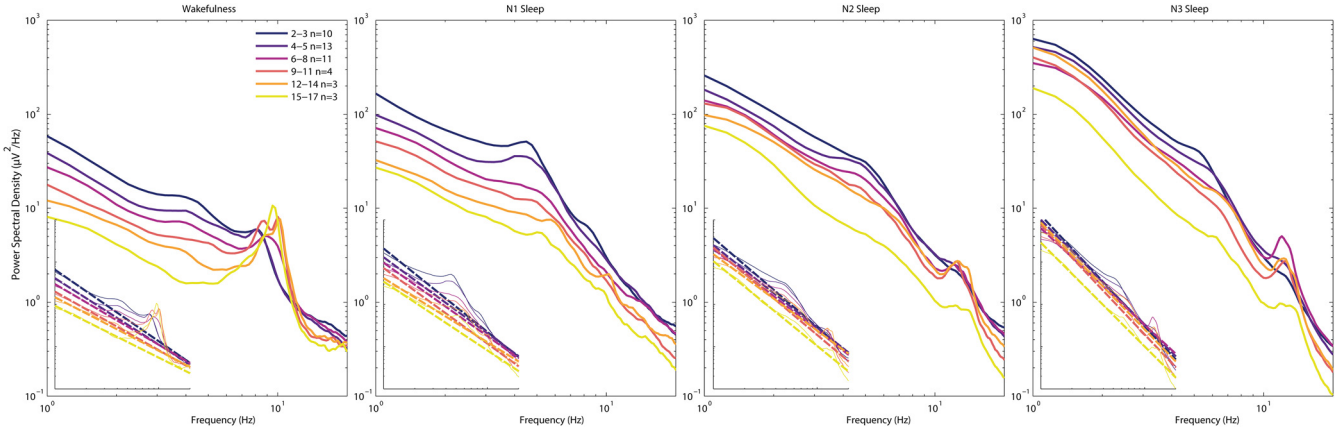

Fig. 2. In each age group, deeper NREM sleep stages implied a clockwise rotation of the PSD, indexed by higher spectral exponent and higher offset. The geometric mean of the 1–20 Hz PSD is taken first across electrodes, then across subjects that belonged to the same age group (numerosity is shown in the legend of the first panel); grouping was performed for visual display only. The subpanels display the PSD along with their 1/f-like trend, corresponding to the average fit of the aperiodic component. A corresponding figure relative to the 1–40 Hz PSD is shown in the Supplementary material (**Supplementary Fig. 14)**.

Table 1
Spearman Correlations between aperiodic features and the vigilance stages (ranked according to the order: Wake, N1, N2, N3). Correlation analysis was performed by pooling the four vigilance stages on the subset of subjects who reached N3 sleep.

	Spearman rank-correlation with vigilance stages	
Aperiodic Feature	Rho (174)	P
Spectral Exponent 1–20 Hz	**0.8672**	**1.4 e-54**
Spectral Offset 1–20 Hz	**0.8794**	**5.52 e-58**
Spectral Exponent 1–40 Hz	**0.9334**	**2.5 e-79**
Spectral Offset 1–40 Hz	**0.8886**	**8.36 e-61**

through N1, N2, to N3; (Rho=0.867; d.f. =42, $P < 0.001$ [$p = 1.4^{-54}$] Fig. 3A, Table 1). Similarly, the spectral offset of the 1–20 Hz range progressively increased from wakefulness to deep sleep (Rho= 0.879, $P < 0.001$ [$p = 5.52^{-58}$]) (Fig. 3C). Similar yet stronger results were obtained for the spectral exponent and offset of the 1–40 Hz range (Rho=0.934, $P < 0.001$ [$p = 2.5^{-79}$] - Rho=0.888, $P < 0.001$ [$p = 8.36^{-61}$] respectively, Table 1, Supplementary Fig. 13).

Notably, regardless of age, both spectral exponent and offset of the 1–20 Hz range entirely separated wakefulness from N3 sleep (Fig. 3) While the spectral offset of the 1–40 Hz range nearly separated wakefulness from N2 and N3 (40/44 and 44/44 respectively), the spectral exponent of the 1–40 Hz range entirely separated wakefulness from both N2 and N3 sleep (Supplementary Fig. 15), with a cutoff near 2, as noted also in a recent study by Schneider et al. (2022).

3.3. Development of aperiodic activity, in each vigilance stage

We evaluated the development of aperiodic activity during wake and sleep. The spectral exponent of the 1–20 Hz range linearly decreased with age in wakefulness and N1 sleep (Wake R = - 0.795, P<0.001 [$P = 4.43^{-10}$]; N1 R = - 0.603, P<0.001 [$P = 4.38^{-05}$]. D.f. 42), but not in N2 nor in N3 sleep (N2 R = - 0.246, P = 0.213; N3 R = - 0.089, P = 0.563). On the other hand, the spectral offset linearly decreased with age, in every sleep stage (N1 R = - 0.782, P<0.001 [$P = 1.07^{-09}$]; N2 R = - 0.560, P<0.001 [P = 0.000152]; N3 R = - 0.402, P = 0.007) (Fig. 3 and Table 2). For both aperiodic features, the correlations with age were stronger during wakefulness and light sleep; correlations in sleep were stronger in the occipital region (Fig. 3B, and D). Similar results were obtained for the aperiodic features of the 1–40 Hz range (Supplementary Fig. 15 and Supplementary Table 9). Overall, the magnitude of the correlations between age and the aperiodic features were greater in wakefulness than in sleep, and progressively decreased with the vigilance stage, from wakefulness, through N1 and N2 to N3 (Supplementary Material, par. **Evaluation of differences between wake and sleep stages in the magnitude of the correlations of age with aperiodic and spatial features**).

Spectral exponent and spectral offset had a similar correlation with age during wakefulness, however, the spectral exponent was less correlated with age than the spectral offset during sleep, as confirmed by bootstrap analysis on the difference in the correlation magnitude (Supplementary Material, par. **Evaluation of differences between aperiodic features in the magnitude of their correlations of age**).

Further, we performed an additional control analysis, to show that the different amount of data available per subject was not driving the observed results (Supplementary Material, par. **Data cleaning and control for potential biases across age**); hence, we subsampled the available data to equate recording lengths across subjects, and observed highly consistent estimates of the aperiodic features (Supplementary Fig. 7), along with the previously described pattern of correlations throughout vigilance stages.

Overall, development rotated the PSD counterclockwise during wakefulness and light sleep, while it only reduced the PSD across frequencies during deep sleep.

3.4. Development of the postero-anterior gradient in each vigilance stage

We evaluated the development of the postero-anterior gradient of aperiodic activity during wake and sleep (Fig. 4). The posterior-to-anterior difference of the spectral exponent of the 1–20 Hz range negatively correlated with age throughout vigilance stages, particularly during deep sleep (Fig. 4 and Table 2; Wake R = - 0.388, P = 0.00925; N1 R = - 0.546, P<0.001 [P = 0.000256]; N2 R = - 0.706, P<0.001 [$P = 3.39^{-07}$]; N3 R = −0.596, P<0.001 [$P = 5{,}91^{-05}$]). Similarly, the posterior-to-anterior difference of the spectral offset of the 1–20 Hz range negatively correlated with age during sleep, particularly during deep sleep (Supplementary Fig. 17; Wake R = −0,169, P = 0.274; N1 R = −0.521, P<0.001 [P = 0,000,573]; N2 R = −0,705, P<0.001 [$P = 3{,}68^{-07}$]; N3 R = −0,621, P<0.001 [$P = 2{,}03^{-05}$]). During wakefulness, correlations of the posterior-to-anterior difference of the spectral offset (1–20 Hz) with age were significant across all subjects (Supplementary Fig. 16), yet these were not significant when considering only the subset of subjects that reached N3 sleep (Supplementary Fig. 17).

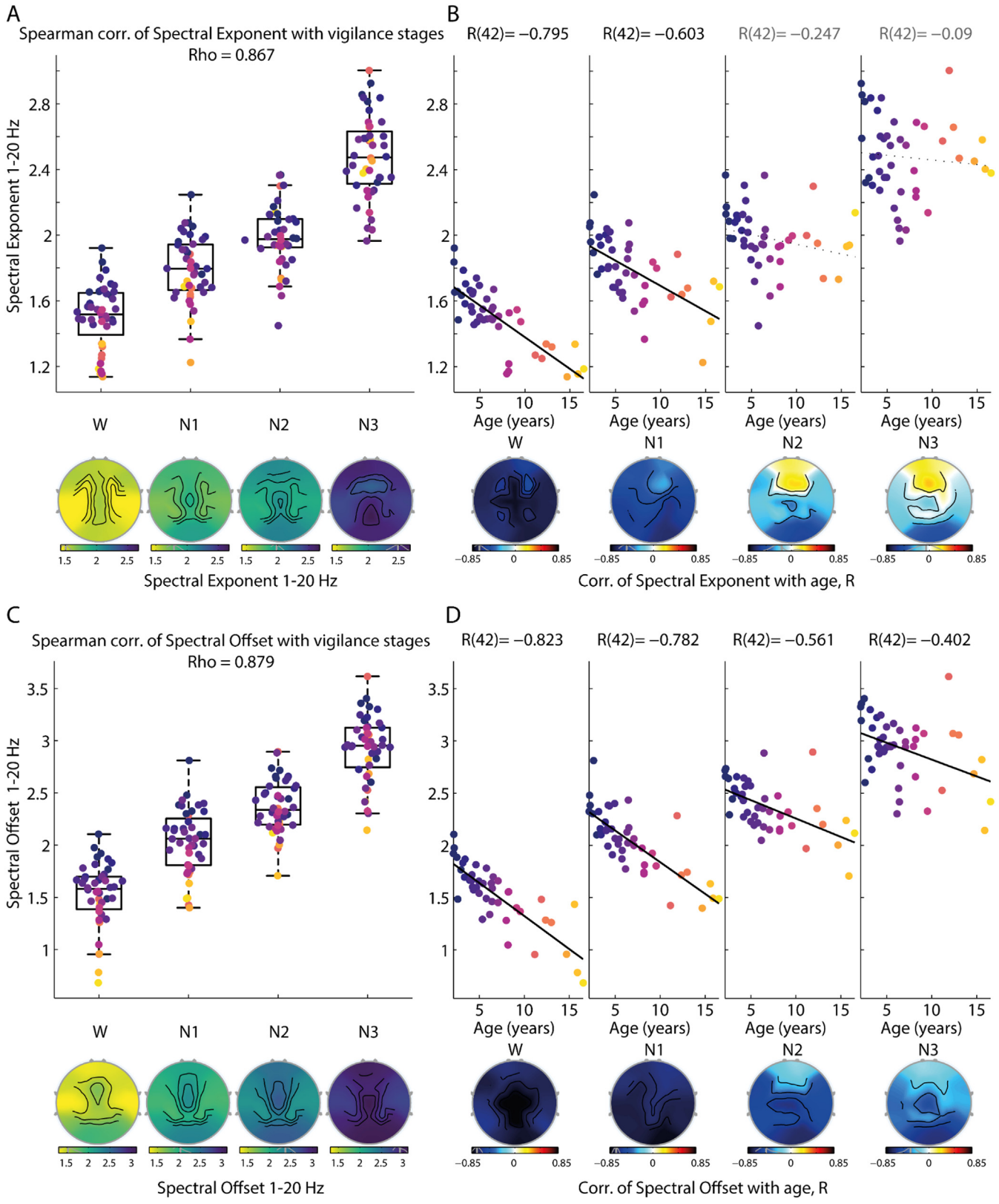

Fig. 3. Overall, aperiodic activity indexed vigilance stage, with higher spectral exponent and offset in deeper sleep; in deep sleep, only the spectral offset progressively decreases over age. Panels A and C: both spectral exponent and offset, estimated over the 1–20 Hz range, progressively increased from Wakefulness, through N1, N2, to N3, as quantified by the Rho values of the Spearman correlation with the vigilance stages (ranked according to the order: W, N1, N2, N3). Regardless of age, spectral features entirely separate wakefulness from N3 sleep. While the spectral offset linearly decreases with age in every sleep stage (panel D), the spectral exponent shows a negative linear correlation with age only in Wakefulness and N1 sleep (panel B). The R-values of the Pearson correlation with age is reported, in gray for non-significant tests. In the lower part of figure A and C, topographies show the spatial distribution of spectral exponent and offset, respectively. Instead, in figure B and D topographies show the spatial distribution of the magnitude of the correlations, performed at the single electrode level.
Wakefulness values reported in this figure are sampled from the subpopulation of subjects that reached N3 ($N = 44$).

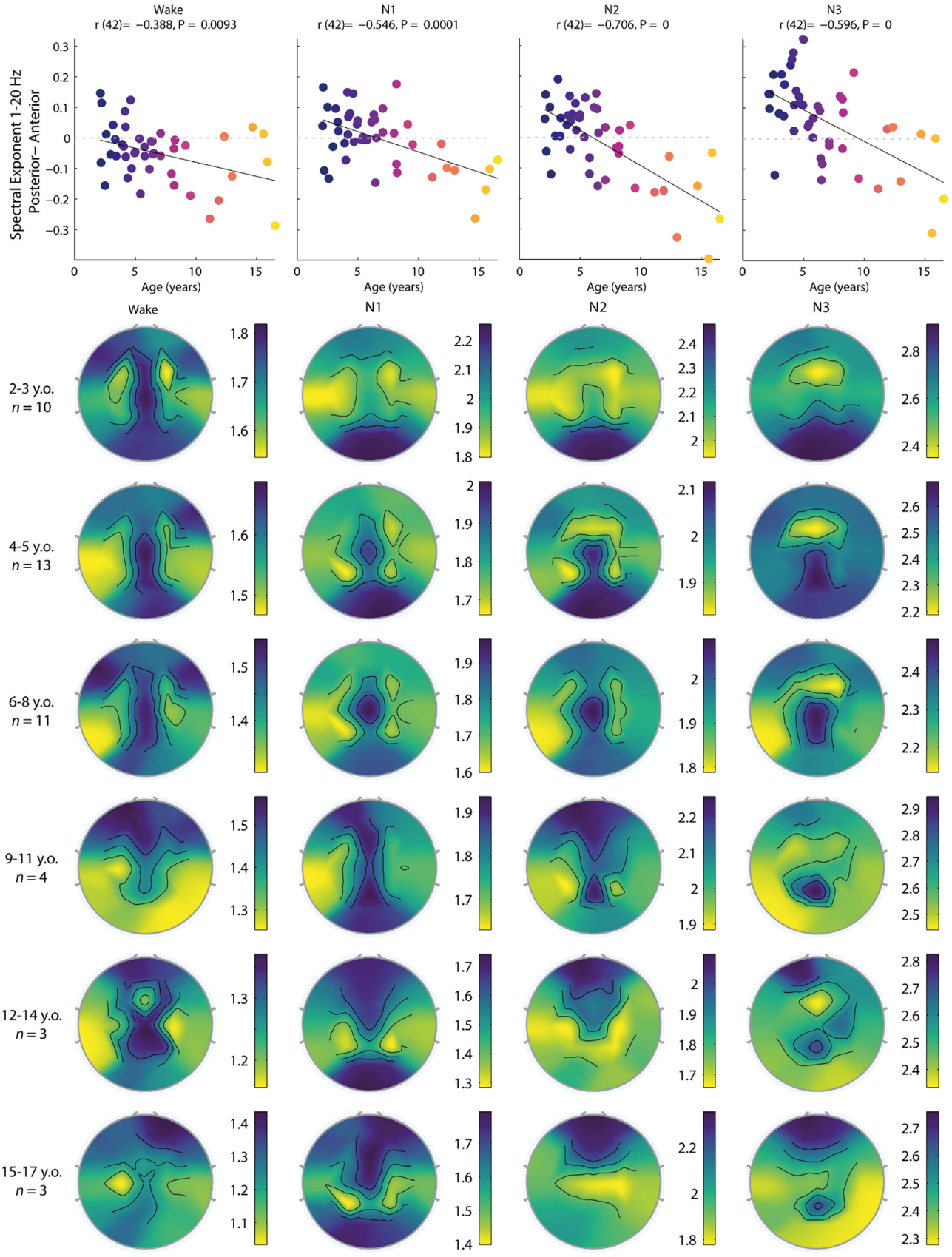

Fig. 4. Throughout vigilance stages, the posterior-to-anterior difference of the spectral exponent negatively correlates with age and the location with higher values of spectral exponent migrates from posterior to anterior regions from childhood to adolescence. Correlation between age and posterior-to-anterior difference of spectral exponent in wakefulness and sleep stages. Color coded topographies display the distribution of spectral exponent over the scalp across vigilance stages, averaged within groups of subjects of different age ranges. The region with steeper spectral exponent is color coded in blue, within each topography.

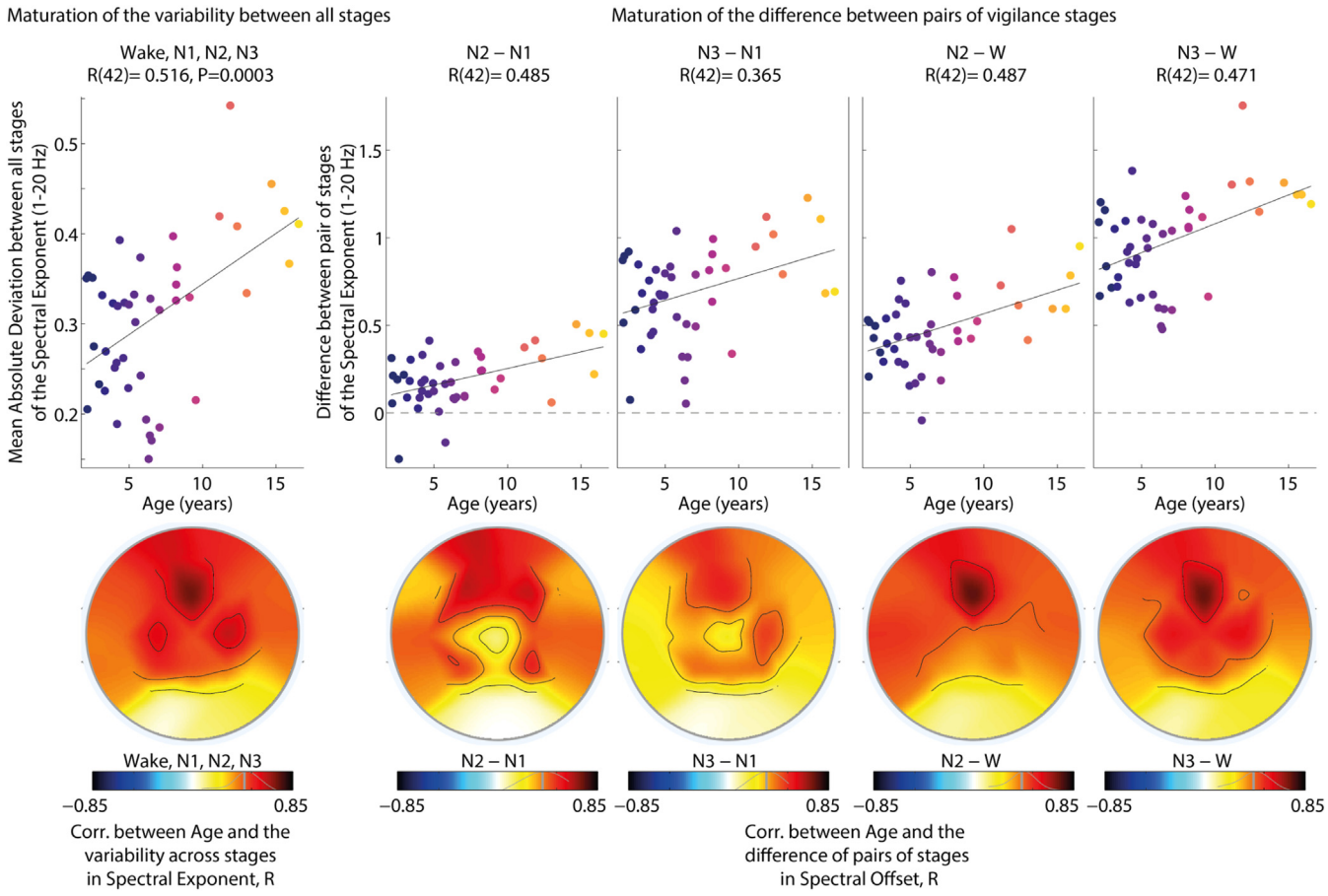

Fig. 5. Over development the values of 1–20 Hz spectral exponent in wakefulness and light sleep became increasingly different from those in deep sleep. Panel above: age correlated with the variability between all the vigilance stages in the spectral exponent of the 1–20 Hz range (computed as the mean absolute deviation of the values between stages, thus an estimate of the overall differentiation between stages). Age was also correlated with most of the pairwise differences in spectral exponent (N2-N1, N3-N1, N2-W, N3-W, except for N1-W and N3-N2, Supplementary Material), indexing a developmental differentiation of wake and light sleep from deep sleep. Panel below: the correlation between age and the variability across vigilance stages in spectral exponent is stronger in frontal regions, similarly to the correlation between age and the pairwise differences between wake and sleep stages in spectral exponent.

Table 2

Correlations between age and spectral features estimated over the 1–20 Hz range for their scalp average and their posteroanterior difference. Correlation analysis across vigilance stages was performed on the subset of subjects who reached N3 sleep; accordingly, the degrees of freedom for the correlations were 42. Abbreviations: p raw = p for individual tests, not adjusted for multiple comparisons. p adj = p adjusted for multiple comparisons across all vigilance stages according to the Bonferoni-Hochberg procedure. *W* = wakefulness. N1 = N1 sleep stage. N2 = N2 sleep stage. N3 = N3 sleep stage. Statistically significant results are marked in bold.

Scalp Average	Pearson correlations with age				
	Stage	W	N1	N2	N3
Spectral Exponent 1–20 Hz	**R**	**−0,7955**	**−0,60,332**	−0,24,673	−0,08,959
	P raw	**1,11E-10**	**1,46E-05**	0,106,404	0,563,043
	P adj	**4,43E-10**	**4,38E-05**	0,212,807	0,563,043
	Stage	W	N1	N2	N3
Spectral Offset 1–20 Hz	**R**	**−0,82,252**	**−0,78,232**	**−0,56,052**	**−0,40,241**
	P raw	**7,49E-12**	**3,57E-10**	**7,59E-05**	**0,006,769**
	P adj	**3E-11**	**1,07E-09**	**0,000,152**	**0,006,769**
PosteroAnterior Difference	Pearson correlations with age				
	Stage	W	N1	N2	N3
Spectral Exponent 1–20 Hz	**R**	**−0,38,803**	**−0,54,555**	**−0,70,633**	**−0,59,595**
	P raw	**0,00,925**	**0,000,128**	**8,46E-08**	**1,97E-05**
	P adj	**0,00,925**	**0,000,256**	**3,39E-07**	**5,91E-05**
	Stage	W	N1	N2	N3
Spectral Offset 1–20 Hz	**R**	−0,16,864	**−0,52,116**	**−0,70,497**	**−0,6213**
	P raw	0,273,832	**0,000,286**	**9,19E-08**	**6,78E-06**
	P adj	0,273,832	**0,000,573**	**3,68E-07**	**2,03E-05**

Table 3
Correlations between age and the difference between pairs of vigilance stages, in aperiodic features of the 1–20 Hz range, reveal a differentiation of wake and light sleep activity from deep sleep activity. Correlation analysis of the pairwise differences between vigilance stages was performed on the subset of subjects who reached N3 sleep; accordingly, the degrees of freedom for the correlations were 42. Bold is used for statistically significant tests, after controlling for multiple comparisons across the 6 pairs of stages. Abbreviations: P raw = P for individual tests, not adjusted for multiple comparisons. P adj = P adjusted for multiple comparisons across all vigilance stages according to the Bonferoni-Hochberg procedure. *W* = wakefulness. N1 = N1 sleep stage. N2 = N2 sleep stage. N3 = N3 sleep stage.

	Stage	N2 - N1	N3 - N1	N1 - W	N3 - N2	N2 - W	N3 - W
Spectral Exponent 1 20 Hz	**R**	**0,484,875**	**0,365,369**	0,187,355	0,107,341	**0,487,348**	**0,47,096**
	P raw	**0,000,851**	**0,014,737**	0,223,296	0,487,976	**0,000,793**	**0,001,253**
	P adj	**0,004,759**	**0,04,421**	0,446,591	0,487,976	**0,004,759**	**0,005,012**
	Stage	N2 - N1	N3 - N1	N1 - W	N3 - N2	N2 - W	N3 - W
Spectral Offset 1 20 Hz	**R**	**0,492,829**	**0,362,437**	0,047,818	0,05,399	**0,504,964**	**0,447,086**
	P raw	**0,000,677**	**0,015,616**	0,757,906	0,727,785	**0,000,473**	**0,002,346**
	P adj	**0,003,386**	**0,046,849**	1	1	**0,002,836**	**0,009,382**

Concerning the posterior-to-anterior differences of both features, bootstrap analysis suggested a progressive decrease of the correlations with age from wake to deeper sleep stages (Supplementary Fig. 4, even though pairwise comparison between wake and each sleep stage revealed that correlations were only marginally greater in Wakefulness than in N2 for the spectral exponent, and greater in Wakefulness than in either N2 or N3 for the spectral offset (see details in Supplementary Material par. **Evaluation of differences between wake and sleep stages, in the magnitude of the correlations of age with aperiodic and spatial features**).

Overall, the location with higher spectral exponent and offset values undergoes a shift from posterior to anterior regions from childhood to adolescence, particularly during sleep (Fig. 4, Supplementary Figs. 16 and 17).

3.5. Development of differences and variability between vigilance stages in aperiodic features

We evaluated the developmental differentiation among vigilance stages in the aperiodic features, considering the overall variability across stages and the pairwise difference between stages.

The variability between all the vigilance stages in the spectral exponent of the 1–20 Hz range linearly correlated with age ($R = 0.516$, d.f.=42, $P<0.001$ [$P = 0.0003$] Fig. 5). Similar results were obtained with regard to the spectral offset of the 1–20 Hz range ($R = 0.536$, Supplementary Fig. 19) and with regard to the spectral features of the 1–40 Hz range (Supplementary Table 11), thus revealing a progressive differentiation of aperiodic features among vigilance stages from infancy to adolescence (Fig. 5).

Specifically, age was significantly correlated with the difference in spectral exponent of the 1–20 Hz range between the following pairs of vigilance stages: N3-W ($R = 0.471$, $P = 0.005$), N3-N1 ($R = 0.365$, $P = 0.044$), N2-W ($R = 0.487$, $P = 0.005$), N2-N1 ($R = 0.485$, $P = 0.005$), see Fig. 5, Table 3; yet, age was not significantly correlated with the difference between N1-W ($P = 0.447$) and N3-N2 ($P = 0.488$) (Supplementary Fig. 18, Table 3). Highly consistent results were obtained for the correlations of age with the pairwise differences between stages in spectral offset of the 1–20 Hz range N3-W ($R = 0.447$, $P = 0.009$), N3-N1 ($R = 0.362$, $P = 0.047$), N2-W ($R = 0.505$, $P = 0.002$), N2-N1 ($R = 0.493$, $P = 0.003$) (Supplementary Fig. 19, Table 3). Results relative to the 1–40 Hz range are reported in Supplementary Table 11).

Concerning topography, correlations of age with both variability and pairwise differences in aperiodic features of the 1–20 Hz range were stronger in frontal regions (Fig. 5, Supplementary Figs. 18 and 19). Overall, aperiodic features of the 1–20 Hz range during both wakefulness and light sleep became progressively different from those in deep sleep.

4. Discussion

Here, we observed a counterclockwise PSD rotation during wakefulness and light sleep from childhood to adolescence, reflecting a reduction in signal amplitude and an increasing representation of fast over slow frequency activity. The PSD rotation was indexed by a decrease in both spectral exponent and offset, for which we report average values for each year of age during wakefulness (Supplementary Table 1). Regardless of age, the broad-band spectral exponent could track sleep depth, entirely discriminating wakefulness from deep sleep (N2 and N3 stages). Further, while the spectral offset decreased with age throughout all vigilance stages, the spectral exponent remained relatively constant with age during deep sleep. In turn, aperiodic activity during wake and light sleep differentiated from activity during deep sleep, thereby the variability across vigilance stages increased over development. Finally, we observed a topographical maturation of both aperiodic features along a posterior to anterior direction, occurring more prominently during deep sleep.

4.1. Maturation of aperiodic activity during wakefulness

During wakefulness, we observed a counterclockwise rotation of the EEG PSD in a large cohort of healthy children and adolescents aged between 2 and 17 years, covering each year of age (Fig. 1). Specifically, age was strongly and linearly correlated to both spectral exponent and offset, respectively reflecting an increase in fast relative to slow frequency activity and an overall reduction of amplitude (Fig. 1).

Similarly, in a large sample of healthy subjects aged 3–24 years, age linearly correlated to both spectral exponent and offset (Cellier et al., 2021), although we observed stronger correlations in our datasets, possibly due to a more homogeneous sampling over age.

We observed a tight linear relation during wakefulness throughout all the years we investigated, in contrast to McSweeeny et al. (2023) who observed a quadratic relationship in middle childhood (4–11 years), although the distribution of values reported is compatible to the one we observed here. Subtle deviations from the overall developmental linear trend may be more evident when focusing on a restricted age group with an even larger dataset (McSweeny et al., 2023). The distribution and trend that we observed from infancy to adolescence are consistent with distributions and trends observed in even younger infants and in adults.

Specifically, spectral exponent values decreased from 3 to 2 during development over the first seven months of life (Schaworonkow and Voytek, 2021). These values are in continuity with the limits of our distribution, whereby toddlers aged 2 displayed a maximum of 1.92 and an average of 1.73 (Supplementary Table 1).

On the other hand, in adult populations the spectral exponent decreases with age as well. Values were distributed between 1.5 and 0.5, with a greater density around 1 (Voytek et al., 2015; Colombo et al., 2019; Donoghue et al., 2020; Pathania et al., 2022). Overall, the PSD rotation that we observed in wakefulness during development, indexed by a reduction of spectral exponent and offset values, is consistent with previous literature.

4.2. The spectral exponent indexes sleep depth and separates wakefulness from deep sleep, regardless of age

Our data demonstrate that PSD gradually rotates clockwise with sleep depth from wake through N1 and N2 to N3 (homogeneously across statistical descriptors), as previously reported in adults (Miskovic et al., 2019) and consistently in different age groups, including children, teenagers, young adults and middle-aged adults (Schneider et al., 2022; Bódizs et al., 2021).

Both spectral exponent and offset values of the 1–20 Hz range entirely separated wakefulness from N3 sleep (Fig. 3); further, spectral offset and exponent values of the 1–40 Hz range separated wakefulness from both N2 and N3 sleep, leading to near-optimal and optimal separation respectively (Supplementary Fig. 15). Overall, the spectral exponent of the 1–40 Hz range demonstrated the strongest monotonic relation with the progression of vigilance stages (W, N1, N2, N3, Table 1).

These results are in line with those obtained in adults during both physiological sleep (Miskovic et al., 2019) and during pharmacologically induced unconsciousness, by xenon or propofol anesthesia (Colombo et al., 2019). However, since periodic and aperiodic EEG activity dramatically develops in the first months of life (Schaworonkow and Voytek, 2021; Mizrahi and Hrachovy, 2016), and since wake EEG aperiodic activity progressively differentiate from sleep activity over development (as shown above), EEG aperiodic activity may be less effective in discriminating wakefulness from sleep in the first year of life.

4.3. Maturation of spectral offset across vigilance stages

Our data showed that the spectral offset linearly decreased with age in every vigilance stage, reflecting a global power reduction during development. This power reduction has been related mainly to synaptic pruning (Whitford et al., 2007), since lower synaptic density is expected to yield lower EEG amplitude. Further, as early as 1982, Feinberg linked previous postmortem evidence to sleep developmental neurophysiology, proposing that lower synaptic density should lead to lower EEG slow-wave amplitude (Feinberg, 1982).

Furthermore, not only the amount of neuronal activity but also its temporal pattern affects neuronal survival rates (Blanquie et al., 2017; Wong Fong Sang et al., 2021). In fact high-frequency activity plays an important role in the stabilization and pruning of synaptic connections (Warm et al., 2022).

Alternatively, the progressive increase over development of the scalp-to-cortex distance (Fu and Richards, 2021; Sharma et al., 2020; Delye et al., 2015) may partially explain the observed reduction in EEG amplitude over development. However, the region-specific and stage-dependent effects that we observed may be harder to explain under this alternative hypothesis. Further, on the basis of this alternative hypothesis, the skull should act as a low-pass filter (Srinivasan et al., 1996), and thus one would expect a steeper spectral exponent over age. Yet, we observed an opposite effect of age during wakefulness and light-sleep, namely a flatter spectral exponent over age, thus implying that the observed effects on EEG aperiodic activity likely reflect genuine neurophysiological maturation.

4.4. Developmental trajectories of spectral exponent and offset

Whereas a reduction in spectral offset can occur in absence of a change in spectral exponent (PSD shift), a flatter spectral exponent also results in a concomitant reduction of the spectral offset, if the PSD is rotating at any non-zero frequency; thus leading in principle to a high correlation between the two aperiodic features.

Despite the observed high mutual correlation between aperiodic features across vigilance stages (Supplementary Fig. 2), the correlation of age with the spectral offset was significantly higher than with the spectral exponent during sleep (Supplementary Material).

Further, during wake and N1 sleep, both spectral exponent and offset decreased over age, whereas during N2 and N3 sleep, despite a reduction of the spectral offset with age, the spectral exponent did not correlate with age (Fig. 3B).

Noteworthy, an effect of age on the exponent might have been observed in NREM sleep, if considered as a whole (N2+N3), but this effect could simply be explained by the reduction of the prevalence of N3 during development (Ohayon et al., 2004).

To control for developmental differences in the duration of sleep stages, we additionally subsampled the data available, retaining the same length of data across ages, and observed highly consistent estimates of the aperiodic features (Supplementary Fig. 7), along with the previously described pattern of correlations throughout vigilance stages (Wake, N1, N2, N3, Supplementary Material, par. **Data cleaning and control for potential biases across age)**.

Overall, during wakefulness and light sleep development induces a counter-clockwise rotation of the EEG PSD, while during deep sleep development primarily induces a PSD shift.

Thus, the spectral exponent and offset, albeit typically strongly correlated, follow distinct developmental trajectories across vigilance stages and index distinct neurophysiological processes.

4.5. Spectral exponent and the development of excitation and inhibition

The study of the aperiodic activity may potentially offer some insights into the cortical balance between excitation and inhibition (Colombo et al., 2019; Gao et al., 2017). The computational model from Gao et al. indicates that inhibitory activity, characterized by slow synaptic currents (Gupta et al., 2000; Bartos et al., 2002) and excitatory activity, characterized by fast synaptic currents (Spruston et al., 1995; Angulo et al., 1999, see for a compendium http://compneuro.uwaterloo.ca/research/constants-constraints/neurotransmitter-time-constants-pscs.html#), have a different spectral decay, such that they primarily weigh respectively on the shape of the low and high frequency range of the spectrum of Local Field Potentials (LFP) recordings (Gao et al., 2017). In turn, the slope of the LFP, estimated on a relatively high frequency range (30–50 Hz), is indicative of the ratio between excitation and inhibition, as supported by additional evidence from primate and rat animal models (Gao et al., 2017).

However, several differences need to be considered when drawing parallels across these studies. Gao et al., 2017, considers simulated and real recordings of intracranial LFP, thus their results concern a smaller spatial scale, do not suffer from scalp blurring properties and are free from EMG confounders, which contaminates the EEG high frequency range.

In our case, the spectral slope of a low-frequency range of the EEG spectrum (1–20 Hz, 1–40 Hz) may thus potentially reflect primarily the influence of slow inhibitory currents, suggesting that a developmental flattening of the slope may index decreased time constants. Consistently, the structural and functional maturation of the inhibitory receptors

(Rakhade and Jensen, 2009), leads to faster inhibitory synaptic time-constants over development, according to primate in-vitro evidence (Hashimoto et al., 2009); in turn, inhibitory synaptic time-constants directly affect the aperiodic shape of the EEG PSD, as demonstrated by recent simulations (Brake et al., 2021). Overall, the PSD decay of the EEG during wakefulness and light sleep flattens over development, parallelling the maturation of inhibitory synaptic activity.

4.6. Progressive developmental differentiation of wakefulness from sleep aperiodic activity

During neurodevelopment, the variability across vigilance stages in both aperiodic features increased over age, implying a progressive differentiation of wake and light-sleep aperiodic activity from deep-sleep activity (Fig. 5). To the best of our knowledge, this aspect has never been demonstrated before.

Indeed, aperiodic activity during wakefulness and light-sleep underwent a greater developmental change than activity during deep sleep (N2, N3), which was significant for the spectral offset, and non-significant for the spectral exponent (Fig. 3). Overall, our results suggest that the neurophysiological waking state progressively differentiates from the state of deep sleep over the course of development.

Further, correlation analysis revealed that the differentiation of aperiodic activity from wakefulness to sleep was more pronounced over frontal regions, consistently with the notion that frontal regions are the last ones to mature and require the most time to complete maturation (Casey et al., 2005)

4.7. Region-specific changes of sleep aperiodic activity: early maturation of occipital regions, later maturation of frontal

The posterior-to-anterior difference of spectral exponent and offset becomes progressively more negative with increasing age across vigilance stages, particularly in deep sleep (Fig. 4). In particular, the hotspot with the largest spectral exponent and offset undergoes a transition from posterior to anterior regions across development (Fig. 4).

During deep sleep, both spectral exponent and offset were higher posteriorly during infancy and anteriorly during adolescence, consistently with the lower posterior-anterior difference in children as compared to adults found by Schneider et al. (2022).

Consistently, Kurth et al. (2010) showed a developmental migration of the location on the scalp with maximal slow wave activity during NREM sleep. Indeed, Horváth et al. (2022) demonstrated that the classical slow wave activity in both adults and children is tightly related to the spectral exponent and, particularly, to the spectral offset. Aperiodic features and slow wave activity were correlated within sleep cycles, and displayed similar overnight homeostatic dynamics, decreasing over consecutive sleep cycles (Horváth et al., 2022). As a consequence, the postero-anterior maturation of the spectral exponent and offset can be related to the postero-anterior maturation of slow wave activity of NREM sleep.

While the development of aperiodic activity along a posteroanterior gradient during sleep is in line with previous evidence concerning sleep slow waves (Kurth et al., al.,2010), the observed positive correlation of age with the posteroanterior difference in spectral exponent during wakefulness is unexpected and could point to a common mechanism regulating the topographical development of the neurophysiological aperiodic activity across wake and sleep, and awaits further investigation.

The developmental maturation of both aperiodic features (exponent and offset) along a postero-anterior gradient during sleep points to region-specific synaptic downscaling and neuroanatomical development.

Indeed, the intense activity of a particular region during wakefulness is expected to be underlied by intense day-time synaptic potentiation and to lead to large slow-wave activity during sleep, according to the synaptic homeostasis hypothesis (Tononi and Cirelli, 2006). Consistently, in infants the topographical maximum of both aperiodic features during sleep peaked occipitally, where the synaptogenesis and pruning occurs the earliest (Huttenlocher et al., 1982) and indeed the acquisition of occipitally-dependent visual function occurs the earliest (Hensch 2005).

Subsequently, in late childhood and adolescence, the topographical maximum of both aperiodic features during sleep peaked frontally, where synaptogenesis and pruning occurs the latest and indeed the acquisition of frontally-dependent high-order cognitive and executive function occurs the latest (Luna et al., 2004).

Overall, the observed topographical maturation of aperiodic EEG activity is consistent with a progressive functional and anatomical maturation along a posteroanterior direction.

4.8. Limitations

The EEG traces were obtained from outpatient recordings during daytime. As a consequence, only a subset of subjects reached the N3 phase of NREM sleep and REM sleep data were not available. Therefore, it was not possible to homogeneously cover in sleep the different ages (similarly to wakefulness). Further studies are needed to confirm the results obtained in sleep, using larger populations and data recorded during overnight sleep as well as covering homogeneously the different years of age.

We did not analyze separately the eyes-open and the eyes-closed condition during wakefulness; however, the change in aperiodic features is relatively small between the two conditions (Colombo et al., 2019; Mc Sweeney et al., 2021, 2023) compared to the developmental and the vigilance effect reported here. Further, two large studies in children and in adolescents did not find a developmental interaction effect related to eye closure/opening (McSweeney et al., 2021, 2023).

Finally, our montage did not include EOG leads and EMG activity was recorded only at deltoid muscles level; however this did not affect the detection of N1, N2 and N3 sleep epochs, scored according to the AASM criteria (Iber et al., 2007). Concerning N1 sleep, we have not considered slow eye movements, which however may be seen also during eyes closed wake and are thus not discriminative.

5. Conclusions

In conclusion, this comprehensive analysis of the aperiodic component of the EEG signal allowed us to characterize and quantify the neurodevelopmental changes of EEG activity occurring during wakefulness and sleep, from infancy to adolescence. Specifically, the spectral offset decreases over development throughout vigilance stages, reflecting an overall voltage reduction in line with synaptic pruning. On the other hand, the spectral exponent decreases over development only during wakefulness and light sleep, reflecting a flatter PSD decay, consistently with a reduction of synaptic time constants possibly related to the maturation of the inhibitory system. As a consequence, wakefulness seems to progressively emerge from the sleep state during development. Finally, we showed that the hotspot with the steepest PSD decay migrates along a posterior-to-anterior gradient from childhood to adolescence, consistent with a progressive cognitive, functional and anatomical neurodevelopment.

Declaration of Competing Interest

Marcello Massimini is co-founder of Intrinsic Powers, a spin-off of the University of Milan; Simone Sarasso and Mario Rosanova are advisors of the same company. All other Authors do not have any conflict of interest.

Credit authorship contribution statement

Jacopo Favaro: Conceptualization, Validation, Investigation, Resources, Data curation, Writing – original draft, Writing – review &

editing, Visualization. **Michele Angelo Colombo:** Conceptualization, Methodology, Software, Validation, Formal analysis, Data curation, Writing – original draft, Writing – review & editing, Visualization. **Ezequiel Mikulan:** Methodology, Formal analysis, Writing – review & editing. **Stefano Sartori:** Resources, Supervision. **Margherita Nosadini:** Resources. **Maria Federica Pelizza:** Resources. **Mario Rosanova:** Validation, Supervision. **Simone Sarasso:** Conceptualization, Validation, Writing – review & editing. **Marcello Massimini:** Conceptualization, Validation, Supervision. **Irene Toldo:** Conceptualization, Validation, Resources, Supervision.

Data availability

Data will be made available on request.

Acknowledgments and fundings

Thanks to all the children and their parents who made this work possible. Thanks to all the staff of the Pediatric Neurology and Neurophysiology Unit, University of Padua. Thanks to Dr. Simone Ruzzante for his precious help in the recruiting phase. Thanks to dr. Andrea Pigorini and dr. Simone Russo for their inputs and comments during the conceptualization of the study and the writing process.

This work was supported by the European Union's Horizon 2020 Framework Program for Research and Innovation under the Specific Grant Agreement No. 945539 (Human Brain Project SGA3) (to M.M., M.R.), by Fondazione Regionale per la Ricerca Biomedica (Regione Lombardia), Project ERAPERMED2019-101, GA 779282 (to M.R.). This work has been also supported by the Tiny Blue Dot Foundation (to M.M.). J.F. is a PhD student in Developmental Medicine and Healthcare planning Sciences, XXXVII cycle, by Università degli studi di Padova. The research of M.A.C. was partially funded by a postdoctoral scholarship from Fondazione Fratelli Giuseppe Vitaliano, Tullio e Mario Confalonieri.

Supplementary materials

Supplementary material associated with this article can be found, in the online version, at doi:10.1016/j.neuroimage.2023.120264.

References

Afroz, S., Parato, J., Shen, H., & Sue Smith, S. (2016). Synaptic pruning in the female hippocampus is triggered at puberty by extrasynaptic GABA A receptors on dendritic spines. doi:10.7554/eLife.15106.001.

Angulo, M.C., Rossier, J., Audinat, E., 1999. Postsynaptic glutamate receptors and integrative properties of fast-spiking interneurons in the rat neocortex. J. Neurophysiol. 82, 1295–1302.

Ballesteros, M.C., Hansen, P.E., Soila, K., 1993. MR imaging of the developing human brain. Part 2. Postnatal development. Radiographics 13 (3), 611–622. doi:10.1148/RADIOGRAPHICS.13.3.8316668.

Barkovich, A.J., Kjos, B.O., Jackson, D.E., Norman, D., 1988. Normal maturation of the neonatal and infant brain: MR imaging at 1.5 T. Radiology 166 (1 Pt 1), 173–180. doi:10.1148/RADIOLOGY.166.1.3336675.

Bartos, M., Vida, I., Frotscher, M., Meyer, A., Monyer, H., Geiger, J.R.P., et al., 2002. Fast synaptic inhibition promotes synchronized gamma oscillations in hippocampal interneuron networks. Proc. Natl. Acad. Sci. U.S.A. 99 (20), 13222–13227.

Benninger, C., Matthis, P., Scheffner, D., 1984. EEG development of healthy boys and girls. Results of a longitudinal study. Electroencephalogr. Clin. Neurophysiol. 57 (1), 1–12. doi:10.1016/0013-4694(84)90002-6.

Blanquie, O., Kilb, W., Sinning, A., Luhmann, H.J., 2017. Homeostatic interplay between electrical activity and neuronal apoptosis in the developing neocortex. Neuroscience 358, 190–200. doi:10.1016/J.NEUROSCIENCE.2017.06.030.

Bódizs, R., Szalárdy, O., Horváth, C., Ujma, P.P., Gombos, F., Simor, P., Pótári, A., Zeising, M., Steiger, A., Dresler, M., 2021. A set of composite, non-redundant EEG measures of NREM sleep based on the power law scaling of the Fourier spectrum. Sci. Rep. 11 (1). doi:10.1038/s41598-021-81230-7.

Brake, N., Duc, F., Rokos, A., Arseneau, F., Shahiri, S., & Plourde, G. (2021). Aperiodic EEG activity masks the dynamics of neural oscillations during loss of consciousness from propofol. doi:10.1101/2021.10.12.464109.

Buzsáki, G., Draguhn, A., 2004. Neuronal oscillations in cortical networks. Science 304 (5679), 1926–1929. doi:10.1126/SCIENCE.1099745.

Casey, B.J., Tottenham, N., Liston, C., Durston, S., 2005. Imaging the developing brain: what have we learned about cognitive development? Trend. Cogn. Sci. (Regul. Ed.) 9 (3 SPEC ISS), 104–110. doi:10.1016/j.tics.2005.01.011.

Cellier, D., Riddle, J., Petersen, I., Hwang, K., 2021. The development of theta and alpha neural oscillations from ages 3 to 24 years. Dev. Cogn. Neurosci. 50. doi:10.1016/j.dcn.2021.100969.

Cohen Kadosh, K., Krause, B., King, A.J., Near, J., Cohen Kadosh, R., 2015. Linking GABA and glutamate levels to cognitive skill acquisition during development. Hum. Brain Mapp. 36 (11), 4334–4345. doi:10.1002/hbm.22921.

Colombo, M.A., Napolitani, M., Boly, M., Gosseries, O., Casarotto, S., Rosanova, M., Brichant, J.F., Boveroux, P., Rex, S., Laureys, S., Massimini, M., Chieregato, A., Sarasso, S., 2019. The spectral exponent of the resting EEG indexes the presence of consciousness during unresponsiveness induced by propofol, xenon, and ketamine. Neuroimage 189, 631–644. doi:10.1016/j.neuroimage.2019.01.024.

Delye, H., Clijmans, T., Mommaerts, M.Y., vander Sloten, J., Goffin, J., 2015. Creating a normative database of age-specific 3D geometrical data, bone density, and bone thickness of the developing skull: a pilot study. J. Neurosurg. Pediatr. 16 (6), 687–702. doi:10.3171/2015.4.PEDS1493.

Donoghue, T., Haller, M., Peterson, E.J., Varma, P., Sebastian, P., Gao, R., Noto, T., Lara, A.H., Wallis, J.D., Knight, R.T., Shestyuk, A., Voytek, B., 2020. Parameterizing neural power spectra into periodic and aperiodic components. Nat. Neurosci. 23 (12), 1655–1665. doi:10.1038/s41593-020-00744-x.

Donoghue, T., Schaworonkow, N., Voytek, B., 2022. Methodological considerations for studying neural oscillations. Eur. J. Neurosci. 55 (11–12), 3502–3527. doi:10.1111/ejn.15361.

Feinberg, I. (1982). Schizophrenia: caused by a fault in programmed synaptic elimination during adolescence? (Vol. 17, Issue 4).

Fu, X., Richards, J.E., 2021. Investigating developmental changes in scalp-to-cortex correspondence using diffuse optical tomography sensitivity in infancy. Neurophotonics 8 (3). doi:10.1117/1.NPH.8.3.035003.

Gao, R., 2016. Interpreting the electrophysiological power spectrum. J. Neurophysiol. 115 (2), 628–630. doi:10.1152/JN.00722.2015.

Gao, R., Peterson, E.J., Voytek, B., 2017. Inferring synaptic excitation/inhibition balance from field potentials. Neuroimage 158, 70–78. doi:10.1016/J.NEUROIMAGE.2017.06.078.

Gasser, T., Verleger, R., Bächer, P., Sroka, L., 1988. Development of the EEG of school-age children and adolescents. I. Analysis of band power. Electroencephalogr. Clin. Neurophysiol. 69 (2), 91–99. doi:10.1016/0013-4694(88)90204-0.

Gupta, A., Wang, Y., Markram, H., 2000. Organizing Principles for a Diversity of GABAergic Interneurons and Synapses in the Neocortex. Science 287 (5451), 273–278.

Hashimoto, T., Nguyen, Q.L., Rotaru, D., Keenan, T., Arion, D., Beneyto, M., Gonzalez-Burgos, G., Lewis, D.A., 2009. Protracted developmental trajectories of GABAA receptor alpha1 and alpha2 subunit expression in primate prefrontal cortex. Biol. Psychiatry 65 (12), 1015–1023. doi:10.1016/J.BIOPSYCH.2009.01.004.

He, B.J., Zempel, J.M., Snyder, A.Z., Raichle, M.E., 2010. The temporal structures and functional significance of scale-free brain activity. Neuron 66 (3), 353–369. doi:10.1016/J.NEURON.2010.04.020.

Hensch, T.K., 2005. Critical period plasticity in local cortical circuits. Nat. Rev. Neurosci. 6 (11), 877–888. doi:10.1038/nrn1787.

Hill, A.T., Clark, G.M., Bigelow, F.J., Lum, J.A.G., Enticott, P.G., 2022. Periodic and aperiodic neural activity displays age-dependent changes across early-to-middle childhood. Dev. Cogn. Neurosci. 54, 101076. doi:10.1016/J.DCN.2022.101076.

Horváth, C.G., Szalárdy, O., Ujma, P.P., Simor, P., Gombos, F., Kovács, I., Dresler, M., Bódizs, R., 2022. Overnight dynamics in scale-free and oscillatory spectral parameters of NREM sleep EEG. Sci. Rep. 12 (1). doi:10.1038/s41598-022-23033-y.

Huttenlocher, P.R., de Courten, C., Garey, L.J., Van der Loos, H., 1982. Synaptogenesis in human visual cortex - Evidence for synapse elimination during normal development. Neurosci. Lett. 33, 247–252.

Iber, C., Ancoli-Israel, S., Chesson, A.L., Quan, S.F., eds. (2007) The AASM Manual For the Scoring of Sleep and Associated events: rules, Terminology and Technical Specifications, Ed 1. Westchester, IL: American Academy of Sleep Medicine. 33 (1982) 247–252 33 (1982) 247-25.

Kurth, S., Ringli, M., Geiger, A., LeBourgeois, M., Jenni, O.G., Huber, R., 2010. Mapping of cortical activity in the first two decades of life: a high-density sleep electroencephalogram study. J. Neurosci. 30 (40), 13211–13219. doi:10.1523/JNEUROSCI.2532-10.2010.

Kwon, H., Walsh, K.G., Berja, E.D., Manoach, D.S., Eden, U.T., Kramer, M.A., Chu, C.J., 2023. Sleep spindles in the healthy brain from birth through 18 years. Sleep doi:10.1093/SLEEP/ZSAD017.

Lendner, J.D., Helfrich, R.F., Mander, B.A., Romundstad, L., Lin, J.J., Walker, M.P., Larsson, P.G., Knight, R.T., 2020. An electrophysiological marker of arousal level in humans. Elife 9, 1–29. doi:10.7554/eLife.55092.

Luna, B., Garver, K.E., Urban, T.A., Lazar, N.A., Sweeney, J.A., 2004. Maturation of cognitive processes from late childhood to adulthood. Child Dev. 75 (5), 1357–1372. doi:10.1111/J.1467-8624.2004.00745.X.

McSweeney, M., Morales, S., Valadez, E.A., Buzzell, G.A., Fox, N.A., 2021. Longitudinal age- and sex-related change in background aperiodic activity during early adolescence. Dev. Cogn. Neurosci. 52. doi:10.1016/j.dcn.2021.101035.

McSweeney, M., Morales, S., Valadez, E.A., Buzzell, G.A., Yoder, L., Fifer, W.P., Pini, N., Shuffrey, L.C., Elliott, A.J., Isler, J.R., Fox, N.A., 2023. Age-related trends in aperiodic EEG activity and alpha oscillations during early- to middle-childhood. Neuroimage 269. doi:10.1016/j.neuroimage.2023.119925.

Miskovic, V., MacDonald, K.J., Rhodes, L.J., Cote, K.A., 2019. Changes in EEG multiscale entropy and power-law frequency scaling during the human sleep cycle. Hum. Brain Mapp. 40 (2), 538–551. doi:10.1002/hbm.24393.

Mizrahi, E., Hrachovy, R.A., 2016. Atlas of Neonatal Electroencephalography, 4th edition Demos Medical Publishing, LLC.

Ohayon, M.M., Carskadon, M.A., Guilleminault, C., Vitiello, M.V., 2004. Meta-analysis of quantitative sleep parameters from childhood to old age in healthy individuals: developing normative sleep values across the human lifespan. Sleep 27 (7), 1255–1273.
Ostlund, B.D., Alperin, B.R., Drew, T., Karalunas, S.L., 2021. Behavioral and cognitive correlates of the aperiodic (1/f-like) exponent of the EEG power spectrum in adolescents with and without ADHD. Dev. Cogn. Neurosci. 48, 100931. doi:10.1016/J.DCN.2021.100931.
Ostlund, B., Donoghue, T., Anaya, B., Gunther, K.E., Karalunas, S.L., Voytek, B., Pérez-Edgar, K.E., 2022. Spectral parameterization for studying neurodevelopment: how and why. Dev. Cogn. Neurosci. 54. doi:10.1016/J.DCN.2022.101073.
Palva, S., Palva, J.M., 2018. Roles of brain criticality and multiscale oscillations in temporal predictions for sensorimotor processing. Trend. Neurosci. 41 (10), 729–743. doi:10.1016/J.TINS.2018.08.008.
Pani, S.M., Saba, L., Fraschini, M., 2022. Clinical applications of EEG power spectra aperiodic component analysis: a mini-review. Clin. Neurophysiol. 143, 1–13. doi:10.1016/J.CLINPH.2022.08.010.
Pathania, A., Euler, M.J., Clark, M., Cowan, R.L., Duff, K., Lohse, K.R., 2022. Resting EEG spectral slopes are associated with age-related differences in information processing speed. Biol. Psychol. 168. doi:10.1016/J.BIOPSYCHO.2022.108261.
Porges, E.C., Jensen, G., Foster, B., Edden, R.A.E., Puts, N.A.J., 2021. The trajectory of cortical gaba across the lifespan, an individual participant data meta-analysis of edited mrs studies. Elife 10. doi:10.7554/eLife.62575.
Pritchard, W.S., 1992. The brain in fractal time: 1/f-like power spectrum scaling of the human electroencephalogram. Int. J. Neurosci. 66 (1–2), 119–129. doi:10.3109/00207459208999796.
Rakhade, S.N., Jensen, F.E., 2009. Epileptogenesis in the immature brain: emerging mechanisms. Nat. Rev. Neurol. 5 (7), 380–391. doi:10.1038/nrneurol.2009.80.
Schaworonkow, N., Voytek, B., 2021. Longitudinal changes in aperiodic and periodic activity in electrophysiological recordings in the first seven months of life. Dev. Cogn. Neurosci. 47. doi:10.1016/j.dcn.2020.100895.
Schneider, B., Szalárdy, O., Ujma, P.P., Simor, P., Gombos, F., Kovács, I., Dresler, M., Bódizs, R., 2022. Scale-free and oscillatory spectral measures of sleep stages in humans. Front. Neuroinform. 16. doi:10.3389/fninf.2022.989262.
Sharma, S.D., Park, E., Purcell, P.L., Gordon, K.A., Papsin, B.C., Cushing, S.L., 2020. Age-related variability in pediatric scalp thickness: implications for auditory prostheses. Int. J. Pediatr. Otorhinolaryngol. 130. doi:10.1016/J.IJPORL.2019.109853.
Silbereis, J.C., Pochareddy, S., Zhu, Y., Li, M., Sestan, N., 2016. The cellular and molecular landscapes of the developing human central nervous system. Neuron 89 (2), 248. doi:10.1016/J.NEURON.2015.12.008.
Smith, J.R. (2012). The Electroencephalogram During Normal Infancy and Childhood: I. Rhythmic Activities Present in the Neonate and Their Subsequent Development. doi:10.1080/08856559.1938.10533820.
Spruston, N., Jonas, P., Sakmann, B., 1995. Dendritic glutamate receptor channel in rat hippocampal CA3 and CA1 pyramidal neurons. J. Physiol. 482, 325–352.
Srinivasan, R., Nunez, P.L., Tucker, D.M., Silberstein, R.B., Cadusch, P.J., 1996. Spatial sampling and filtering of EEG with spline laplacians to estimate cortical potentials. Brain Topogr. 8 (4), 355–366. doi:10.1007/BF01186911.
Tamnes, C.K., Østby, Y., Fjell, A.M., Westlye, L.T., Due-Tønnessen, P., Walhovd, K.B., 2010. Brain maturation in adolescence and young adulthood: regional age-related changes in cortical thickness and white matter volume and microstructure. Cereb. Cortex 20 (3), 534–548. doi:10.1093/CERCOR/BHP118.
Toga, A.W., Thompson, P.M., Sowell, E.R., 2006. Mapping brain maturation. Trend. Neurosci. 29 (3), 148–159. doi:10.1016/j.tins.2006.01.007.
Tononi, G., Cirelli, C., 2006. Sleep function and synaptic homeostasis. Sleep Med. Rev. 10 (1), 49–62. doi:10.1016/j.smrv.2005.05.002.
Tran, T., Rolle, C., Gazzaley, A., Voytek, B., 2020. Linked sources of neural noise contribute to age-related cognitive decline. J. Cogn. Neurosci. 1–110. doi:10.1162/jocn_a_01584.
Tröndle, M., Popov, T., Dziemian, S., Langer, N., 2022. Decomposing the role of alpha oscillations during brain maturation. Elife 11, e77571. doi:10.7554/eLife.77571.
van Noordt, S., Willoughby, T., 2021. Cortical maturation from childhood to adolescence is reflected in resting state EEG signal complexity. Dev. Cogn. Neurosci. 48, 100945. doi:10.1016/J.DCN.2021.100945.
Varela, F., Lachaux, J.P., Rodriguez, E., Martinerie, J., 2001. The brainweb: phase synchronization and large-scale integration. Nat. Rev. Neurosci. 2 (4), 229–239. doi:10.1038/35067550.
Vélez-Fort, M., Audinat, E., Angulo, M.C., 2012. Central role of GABA in neuron-glia interactions. Neuroscient.: Rev. J. Bring. Neurobiol., Neurol. Psychiatry 18 (3), 237–250. doi:10.1177/1073858411403317.
Voytek, B., Kramer, M.A., Case, J., Lepage, K.Q., Tempesta, Z.R., Knight, R.T., Gazzaley, A., 2015. Age-related changes in 1/f neural electrophysiological noise. J. Neurosci. 35 (38), 13257–13265. doi:10.1523/JNEUROSCI.2332-14.2015.
Warm, D., Schroer, J., Sinning, A., 2022. Gabaergic interneurons in early brain development: conducting and orchestrated by cortical network activity. Frontiers in Molecular Neuroscience, 14. Frontiers Media, S.A. doi:10.3389/fnmol.2021.807969.
Welker, K.M., Patton, A., 2012. Assessment of normal myelination with magnetic resonance imaging. Semin. Neurol. 32 (1), 15–28. doi:10.1055/s-0032-1306382.
Whitford, T.J., Rennie, C.J., Grieve, S.M., Clark, C.R., Gordon, E., Williams, L.M., 2007. Brain maturation in adolescence: concurrent changes in neuroanatomy and neurophysiology. Hum. Brain Mapp. 28 (3), 228–237. doi:10.1002/hbm.20273.
Wong Fong Sang, I.E., Schroer, J., Halbhuber, L., Warm, D., Yang, J.W., Luhmann, H.J., Kilb, W., Sinning, A., 2021. Optogenetically controlled activity pattern determines survival rate of developing neocortical neurons. Int. J. Mol. Sci. 22 (12). doi:10.3390/IJMS22126575. http://compneuro.uwaterloo.ca/research/constants-constraints/neurotransmitter-time-constants-pscs.html#.